



OPEN Patchiness of plankton ecosystem structure due to nutrient mixing along the shelf edge in the North Sea

Axelle Cordier^{1✉}, Jørgen Bendtsen², Niels Daugbjerg³, Nikolaj From¹, Sigrún Huld Jónasdóttir⁴, Erik Askov Mousing⁵, Jens Tang Christensen⁶, Teresa Silva⁷ & Katherine Richardson¹

Mid-water column turbulence has been shown to cause elevated vertical nutrient flux at the shelf edge in the northeastern North Sea. Here, we demonstrate that phytoplankton communities in this region tend to be dominated by larger cells (estimated from percentage of chlorophyll captured on a 10 µm filter) than beyond the shelf edge. F_v/F_m (PSII electron transport capacity) corrected for photoinhibition in the surface layer correlated in this study with the percentage of chlorophyll captured on a 10 µm filter (assumed to be large cells), suggesting that the phytoplankton community was responding to increased nutrients in the euphotic zone by increasing photosynthetic efficiency and altering community composition. The greatest abundances of larger copepods and the highest rates of *Centropages typicus* egg production were also generally found at the shelf edge. These results suggested that impact from increased nutrient fluxes cascaded up the planktonic food web. As these regions of nutrient flux were very localised, this led to sub-mesoscale heterogeneity in plankton ecosystem structure. Reports of higher abundances of fish and mammals at the shelf edge are common and we hypothesise that their distributions are a response to the impact of mid-water column nutrient upwelling on the plankton food web in the region.

An inherent characteristic of vertical and horizontal plankton distributions in marine and freshwater environments is their spatial patchiness^{1,2}. This uneven distribution is often attributed to the interplay between physical (i.e., water movement), chemical (i.e., nutrient availability) and biological factors (i.e., predation)³. It is also often assumed that patchiness in the size distributions of plankton impacts the distribution of organisms populating higher trophic levels⁴. However, a mechanistic understanding of the processes driving the patchiness in the structure of plankton ecosystems is still lacking.

The role of turbulence in the stimulation of primary production in localised areas has been investigated and the potential for phytoplankton patches to influence the upper planktonic food web structures has been argued⁵. Furthermore, field studies frequently report elevated concentrations of zooplankton and fish larvae at marine fronts, leading to speculation that localised vertical mixing could be responsible for small-scale variations in plankton ecosystem structure compared to those found in waters distant from these frontal zones^{6,7}. The specific plankton ecosystems at fronts are thus primary candidates for supporting the enhanced upper trophic levels associated with mixing areas⁸. We therefore expect that localised vertical mixing between nutrient-deplete and nutrient-rich water masses in the euphotic zone will be reflected in plankton food web structure.

The term *new production* (NP) was formulated⁹ to differentiate primary production supported by nitrogen coming from an external source from regenerated primary production, i.e., fuelled solely by nitrogen regenerated within the system. The f-ratio was later defined¹⁰ as the proportion of NP in the total primary production. When primary production is based on locally regenerated nutrients, production may be in an almost stable state and

¹Globe Institute, Section for Biodiversity, University of Copenhagen, Universitetsparken 15, 2100 Copenhagen Ø, Denmark. ²Globe Institute, Section for Geobiology, University of Copenhagen, Øster Voldgade 5-7, 1350 Copenhagen K, Denmark. ³Marine Biological Section, Department of Biology, University of Copenhagen, Universitetsparken 4, 2100 Copenhagen Ø, Denmark. ⁴National Institute of Aquatic Resources, Technical University of Denmark, 2800 Kgs. Lyngby, Denmark. ⁵Department of Climate Modeling and Air Pollution, Norwegian Meteorological Institute, Postbox 43 Blindern, NO-0313 Oslo, Norway. ⁶Department of Biology, Aarhus University, Ole Worms Allé 1, 8000 Aarhus C, Denmark. ⁷Marine Pelagic Division, Marine and Freshwater Research Institute, Fornubudin 5, 220 Hafnafjörður, Iceland. ✉email: axelle.cordier@sund.ku.dk

the *f*-ratio low, while input of nitrate into the euphotic zone can lead to a higher *f*-ratio and a net increase in phytoplankton biomass. Evidence from the permanently stratified Sargasso Sea indicated that where mid-water column vertical mixing occurs, there are hotspots of primary production (PP) with elevated *f*-ratios, and increased concentrations of eel larvae¹¹. In contrast to the Sargasso Sea, the northeastern North Sea is only seasonally stratified. Low PP has traditionally been assumed to take place during the summer period when the water column is stratified. However, turbulence was measured at the shelf edge of the northeastern North Sea and localised vertical mixing was demonstrated¹². A model study additionally showed the potential of this mixing to result in NP hotspots¹³. The region in which these hotspots were predicted to occur coincided with regions where high concentrations of fish larvae were reported¹⁴. Relatively high nitrate fluxes ($>0.5 \text{ mmol N m}^{-2} \text{ d}^{-1}$) were found to be caused by localised vertical mixing along the shelf edge¹², bringing nutrient-rich deep waters into the euphotic zone. At the shelf edge, the nutricline was found to be significantly deeper¹³ and a breach in the stratified water column by localised mixing could explain the relatively high NP ($\sim 100 \text{ mg C m}^{-2} \text{ day}^{-1}$) estimates here. The region in which these localised events were identified is known to house a diverse and abundant fauna including top predators¹⁵.

A relatively short 'traditional' food web characterised by large phyto- and zooplankton can be differentiated⁴ from a relatively long one dominated by smaller organisms. It has been empirically shown that trophic transfer is more efficient when both prey and predator size diversity is higher¹⁶. The diversity and size structure of phytoplankton are thus believed to control how efficiently energy introduced to the food web via photosynthesis is passed on to higher trophic levels. Spawning fish populations are known to aggregate at shelf fronts¹⁷ (e.g. Celtic Sea), possibly due to enhanced food availability (i.e., through an increase in mesozooplankton abundance), and are therefore more intensively fished there^{18,19}. Therefore, in theory, productive areas characteristic of upwelling regions are associated with this specific ecosystem structure (phytoplankton communities dominated by large phytoplankton and relatively efficient transfer of energy through the planktonic food web) resulting in enhanced fish production^{5,20,21}.

Here, we empirically test the hypothesis that the impact of localised subsurface vertical mixing events cascades through the food web and is associated with spatial heterogeneity in plankton ecosystem structure. Using data collected along 5 transects (Fig. 1) on the VERMIX-cruise during July 2016, i.e., the same cruise used to demonstrate elevated vertical mixing in the shelf edge area¹³, we identify water patches in the same area as these mixing events with i) elevated variable fluorescence corrected for photoinhibition²², ii) elevated proportions of large phytoplankton and zooplankton, iii) increased abundance of zooplankton and iv) higher copepod egg production rate than in surrounding waters. These data validate the theory of a cascade effect, triggered by localised subsurface mixing of nutrients into the euphotic zone, up through the plankton food web. The localised mixing events appear to generate sub-mesoscale patchiness in the structure of the plankton ecosystems in the region of the shelf edge.

Results

Primary and secondary producers were sampled in the northeastern North Sea (Fig. 1). As a basis of locating a signal of mixing, we additionally show nitrate flux estimates previously reported¹². Analysis of the vertical distribution of chlorophyll *a* concentration showed a weakening of the deep chlorophyll maximum (DCM) at the shelf edge that spatially coincided with both elevated mixing, higher estimates of nitrate flux and greater heterogeneity in the proportion of large cells in the phytoplankton community

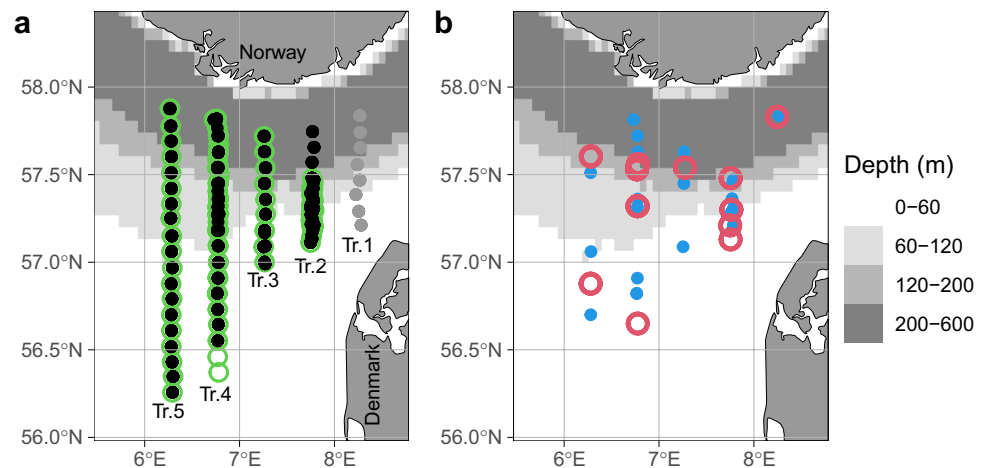


Fig. 1. Position of samples collected at Transect 1–5 in the North Sea, (a) Water samples used for chlorophyll *a* measurement (solid black circles) and stations selected for F_v/F_m measurements (green open circles), Transect 1 (solid grey circles) was excluded from the analyses. (b) Water samples used for egg production rates (blue solid circles) and zooplankton samples (pink open circles). Maps were produced using the ggOceanMaps package²³ in R²⁴.

(proportion of total chlorophyll *a* retained on a 10 μm filter (chlorophyll $a \geq 10 \mu\text{m}/\text{GFF}$), with evident variations among transects in magnitude and spatial relation to nitrate fluxes (Fig. 2). F_v/F_m^* was used as an indication of nutritional status of the phytoplankton community. Elevated F_v/F_m^* in surface waters suggested that phytoplankton here had benefited from increased nutrient enrichment (Fig. 3). F_v/F_m^* at the surface and at the DCM over the entire study area correlated significantly with chlorophyll $a \geq 10 \mu\text{m}/\text{GFF}$ (Fig. 4). A greater proportion of chlorophyll $a \geq 10 \mu\text{m}/\text{GFF}$ was assumed to correspond to a greater dominance of large cells in the phytoplankton community.

Egg production rates (EPR; eggs female⁻¹ day⁻¹) were determined for two copepods, *Centropages typicus* and *Temora longicornis*. EPR for *C. typicus* increased from shallow waters to the shelf edge region (Fig. 5a). The combined EPR data for both copepods were related to the predominance of larger phytoplankton (Fig. 5b) in the water column. Mapping of the distribution of “small” (0.5–1 mm) and “large” (1.5–2 mm) copepods indicated the greatest concentration of the larger copepods to be centered at the shelf edge (Fig. 6).

DCM strength, nutrient fluxes and chlorophyll size fractions

While the southern and northern parts of the study area (Fig. 1), i.e. bottom depths < 60 m and deeper than 120 m, respectively, were generally characterised by the presence of a strong DCM, the chlorophyll *a* concentrations were much more heterogeneously vertically distributed at the intermediate depths along the shelf edge (Fig. 2a). The area in which the weakest DCM was observed coincided with the region (~57.25–57.50°N) in which the largest vertical nutrient fluxes were estimated (Fig. 2b). One station with a weakened DCM was also recorded at the northern end of Transect 4, where factors not associated with shelf-edge processes may be inducing mixing (see below). Thus, the vertical distribution of chlorophyll *a* in the study area appears to reflect the water column turbulence patterns and estimated vertical nutrient fluxes for the area¹³. Furthermore, the strongest signals of the weakened DCM were on Transect 2 and corresponded to nearby stations having the most elevated ratios of chlorophyll $a \geq 10 \mu\text{m}/\text{GFF}$ (Fig. 2c). In addition to the shelf edge, the station at the northern end of Transect 4 exhibiting a weakened DCM was associated with a greater dominance of large phytoplankton in the surface water community than elsewhere on this transect.

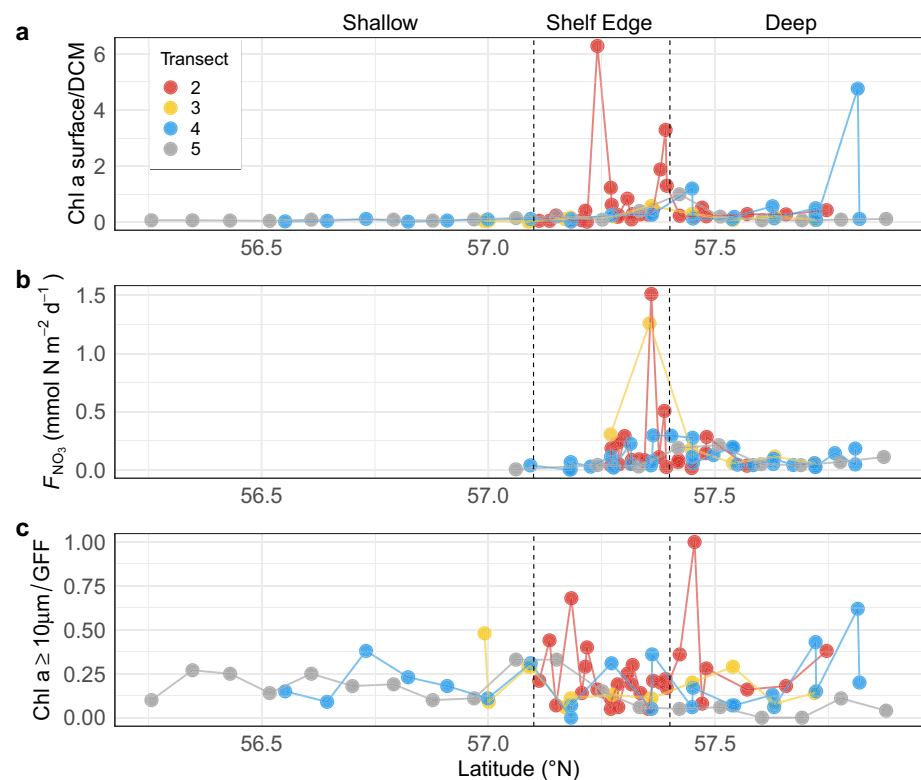


Fig. 2. Measurements of chlorophyll *a* ratios and nitrate fluxes in shallow, shelf edge and deep areas. (a) Ratios of chlorophyll *a* concentration at surface layers (5 m) and DCM, (b) Maximum nitrate flux into the euphotic zone previously reported¹². Note that nitrate was not detectable above the shallow area, i.e., $F_{\text{NO}_3} = 0$. (c) Surface (5 m) ratio of chlorophyll $a \geq 10 \mu\text{m}$ per GFF filter.

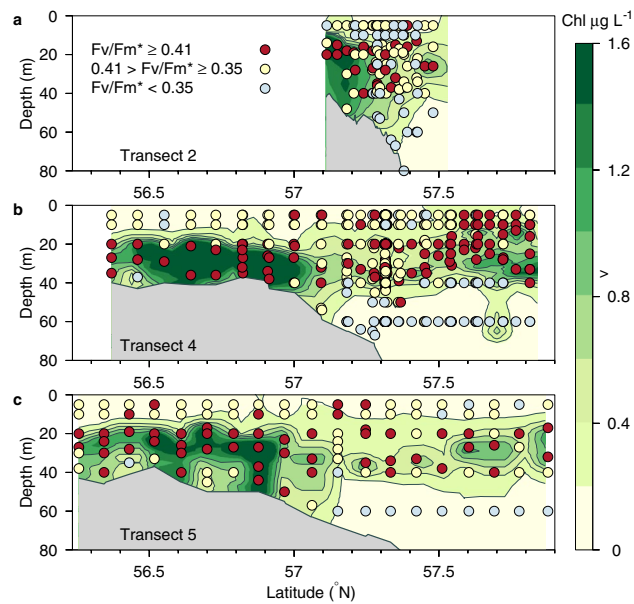


Fig. 3. Distributions of F_v/F_m^* below 0.35 ($< \text{mean} - \text{SD}$), within 0.35–0.41 (within $\text{mean} \pm \text{SD}$) and above 0.41 ($> \text{mean} + \text{SD}$) at three different transects, (a) Transect 2, (b) Transect 4 and, (c) Transect 5. Chlorophyll *a* concentrations are shown as contours (Chlorophyll *a*, $\mu\text{g L}^{-1}$). The figure was made using the scientific graphic language Gri (version 2.12.23, <https://gri.sourceforge.net/>).

Vertical mixing and surface nutrient status

F_v/F_m^* represents electron transport efficiency in PSII and, when corrected for photoinhibition¹⁸, i.e., F_v/F_m^* , it indicates the nutritional status of the phytoplankton community. For simplification, F_v/F_m^* values were categorised into low ($< \text{mean} - \text{SD}$), medium (within $\text{mean} \pm \text{SD}$) and high ($> \text{mean} + \text{SD}$) values. In general, F_v/F_m^* values at the surface (≤ 10 m) were considerably lower than those recorded at the DCM (Fig. 3). This was consistent with the expected nutrient limitation of phytoplankton in the surface layer. Nevertheless, F_v/F_m^* in the surface layer displayed patchiness (Fig. 3).

Relatively high surface F_v/F_m^* values were found at some stations over the shelf edge, i.e., the region where vertical nutrient flux was estimated to be enhanced¹². On Transect 2, the relatively high surface F_v/F_m^* around 57.4°N matched well the strong signal of the DCM weakening, nitrate flux and high proportion of large cells in the phytoplankton community (Fig. 2). On Transect 4, relatively high surface values were also recorded at the northernmost stations of the transect, a region also associated with a weak DCM (Fig. 2a), and where the DCM was closer to the surface than in the remainder of the study area (Fig. 3). This northerly end of the transect was potentially influenced by Norwegian coastal waters, i.e., water outflow from the Baltic Sea¹³. On Transect 5, relatively high surface F_v/F_m^* values were also recorded in the shallowest (southern) part of the transect (~ 40 m), where the shallow depth may explain a relatively larger mixing between surface and bottom layers due to wind and tidal forcing. Thus, the elevated F_v/F_m^* in surface waters suggested that phytoplankton here had benefited from increased nutrient enrichment of the surface waters (Fig. 3).

F_v/F_m^* and phytoplankton size structure

The size structure of the phytoplankton communities (estimated from size fractionated chlorophyll determinations) along all transects at all depths was significantly related to F_v/F_m^* ($p < 0.01$) with communities dominated by large cells having the highest F_v/F_m^* (Fig. 4). Linking this result to F_v/F_m^* distributions (Fig. 3), surface phytoplankton communities dominated by large cells were found at the shelf edge. The combined dataset included samples from the DCM, where communities tended to be more nutrient replete compared to surface waters. The inclusion of the DCM data increased the range of F_v/F_m^* values included in the analysis. Note that ratios higher than 1 were seen from a few samples because filtering was made from independent replicates. Thus, in some cases, higher chlorophyll *a* was observed on larger filter size.

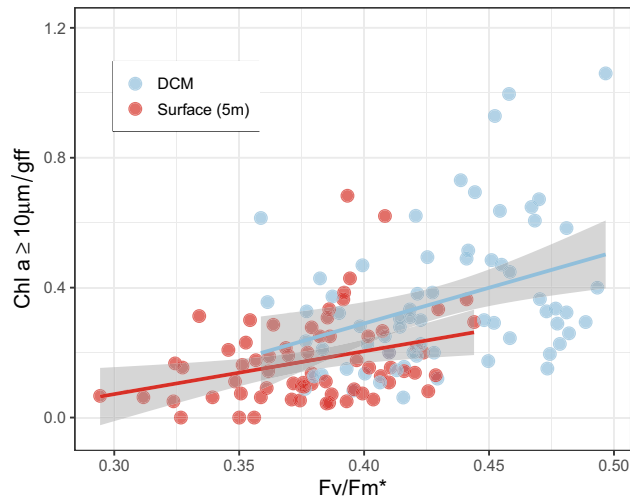


Fig. 4. Relationship between F_v/F_m^* and chlorophyll $a \geq 10 \mu\text{m}/\text{GFF}$ at the surface and DCM of all transects. Linear regressions were fitted to data from all transects, at the surface ($R^2=0.1$, $p < 0.01$) and at the DCM ($R^2=0.16$; $p < 0.001$). Shaded ribbon is the 95% confidence interval.

Copepod egg production and zooplankton distribution

Egg production rates, i.e., EPR (eggs female⁻¹ day⁻¹), were determined for two copepods, *Centropages typicus* and *Temora longicornis*. We found a significant linear relationship ($p < 0.01$) describing an increasing trend in EPR for *C. typicus* from the shallow to the shelf edge area (Fig. 5a). Deep area samples were excluded from the analysis due to a lack of data points between bottom depths ~ 160–300 m. There, the few low values were consistent with the decreased turbulence activity north of the shelf edge, and the relatively high value on transect 4 (bottom depth ~ 353 m; latitude ~ 57.8°N) coincided with a zone exhibiting a weak DCM and high surface F_v/F_m^* (Fig. 2). The highest mean EPR of *C. typicus* was found on Transect 3 in the water column with bottom depths ~ 127 m (Fig. 5a), corresponding to a peak in surface ratios of chlorophyll $a \geq 10 \mu\text{m}/\text{GFF}$ (latitude ~ 57.4°N; Fig. 2).

The EPR of both *C. typicus* and *T. longicornis* were normalised based on the mean and standard deviation: $Z = (EPR - \mu) / \sigma$, where μ is the mean of EPR of both species and σ its standard deviation. A t-test was conducted to assess the difference between the mean normalised EPR found at low (< Median) or relatively high (\geq Median) proportions of chlorophyll $a \geq 10 \mu\text{m}/\text{GFF}$ in the water column. The median

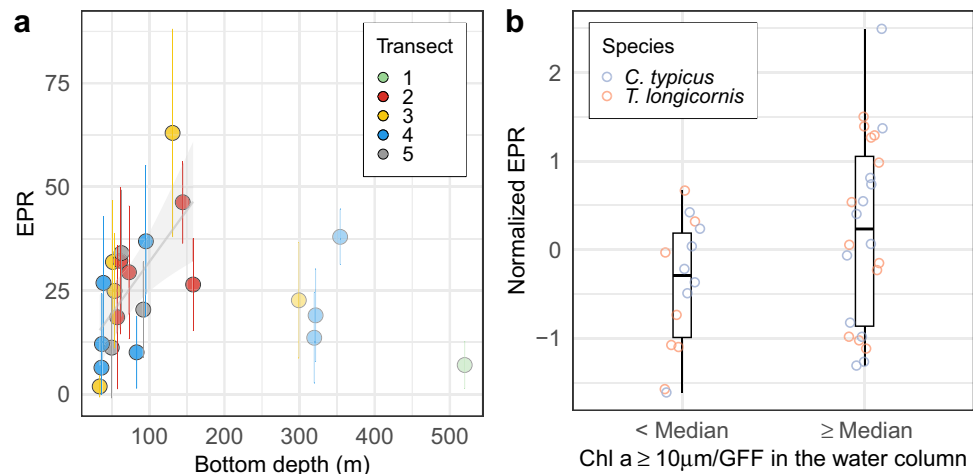


Fig. 5. (a) Average (\pm standard error) of *C. typicus* egg production rate (EPR: eggs female⁻¹ day⁻¹) over bottom depth. A linear regression ($R^2=0.45$, $p < 0.05$) was fitted to the data located at the shallow and shelf edge with 95% confidence interval (shaded ribbon), (b) Box plot of the normalised (Z-score) EPR for two copepod species (*C. typicus* and *T. longicornis*) when mean chlorophyll $a \geq 10 \mu\text{m}/\text{GFF}$ in the water column was below and above the median ($=0.28$) of the entire data set. The box delimits the 25 and 75th percentile, and the whisker is the range. The comparison between the groups' mean was assessed with a t-test ($p < 0.05$).

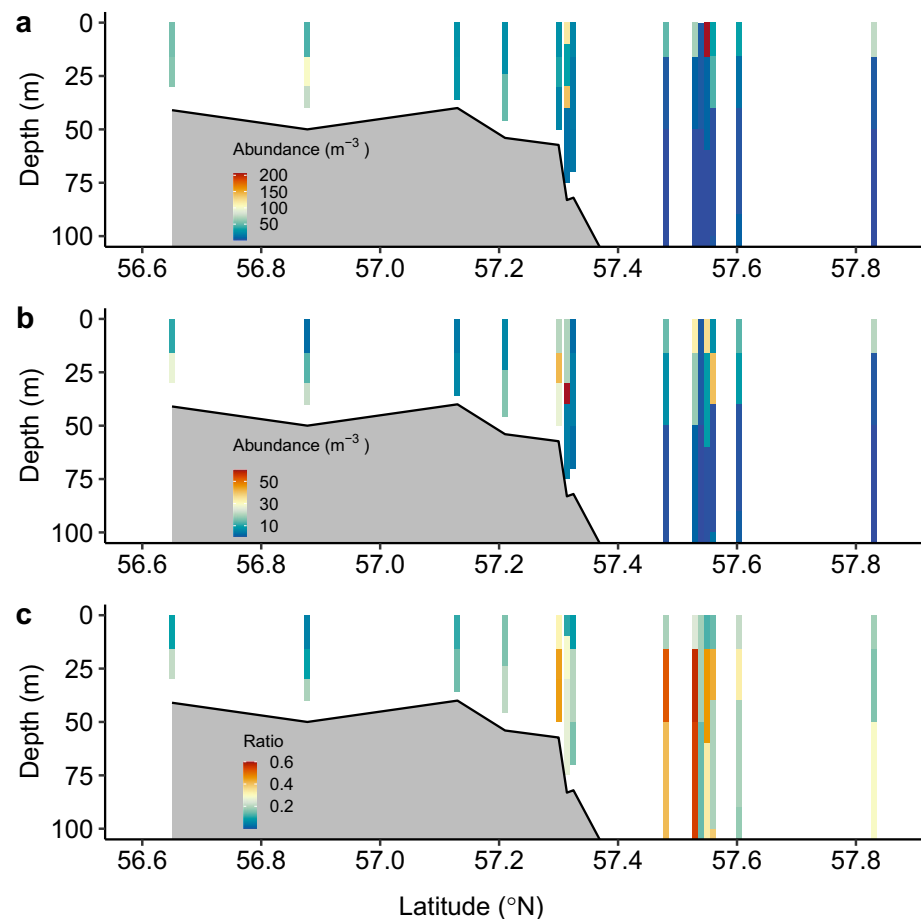


Fig. 6. Mean values of vertical abundance of copepods over all transects, (a) size range 0.5–1 mm, (b) size range 1.5–2 mm and (c) the ratio of the 1.5–2 mm size range over total copepod abundances. The black line represents the bottom depth at the station sampled.

of the chlorophyll $a \geq 10 \mu\text{m}/\text{GFF}$ in the water column was chosen as a threshold to categorise EPR values found in the lower and higher half of chlorophyll $a \geq 10 \mu\text{m}/\text{GFF}$ observations. We found EPR values to be significantly higher ($p < 0.01$) in the presence of relatively high proportions of large phytoplankton.

Communities dominated by smaller (0.5–1 mm) copepods were found over the entire study area, while communities dominated by the larger copepods (1.5–2 mm) were found only in the water column near the shelf edge at $\sim 57.35^\circ\text{N}$ and $\sim 57.5^\circ\text{N}$ (Fig. 6). Most of the copepod species identified (*Calanus*, *Oithona* and *Pseudocalanus*) followed the same pattern, except for *Temora* which seemed to be in lower abundance in the water column at the shelf edge compared to the shallow area (see Supplementary Fig. S2 online).

Discussion

It has long been argued^{4,5} that nutrient enrichment by vertical mixing will lead to greater abundance of large phytoplankton and that this, in turn, will support the production and increase in abundance of mesozooplankton. Empirical demonstration of this cascade is, however, difficult partly because mixing events are often ephemeral but also owing to differences in sampling scales and time lags in responses of the different trophic levels. Directly linking phytoplankton and zooplankton community structure is hampered by the fact that the former is usually sampled at specific depths and the latter over the entire water column or in relatively large depth strata. In addition, water movements are continually transporting organisms during the time it takes for phytoplankton to respond to nutrient enrichment or for zooplankton to respond to changes in phytoplankton community structure. Thus, we may predict that responses in phyto- and zooplankton ecosystem structure to nutrient enrichment will be separated in time and space both from each other and from mixing events themselves.

Here, we take advantage of earlier work^{12,13} demonstrating that episodic vertical turbulent nutrient fluxes from deep to surface waters are more common over the shelf edge in the northeastern North Sea than in the regions to the north and south. Using data collected on the same cruise as these studies, we demonstrated greater heterogeneity in phytoplankton and zooplankton community characteristics in this region with areas with elevated vertical mixing. Furthermore, it was also in this region that we observed evidence of phytoplankton communities dominated by large cells to be present over the entire water column at some stations. These findings were consistent with the hypothesised^{4,5} relationships between nutrient mixing and plankton ecosystems.

That there may be a causal relationship between the mixing and the responses noted in the phytoplankton community was supported by the demonstration of a significant relationship between F_v/F_m^* and the relative proportion of large cells in the community, both at the surface and at the DCM. The finding of a relationship between F_v/F_m^* and the size structure of the phytoplankton community is particularly noteworthy as it may provide a more general tool for assessing relative differences in community size structure.

On land, it is well established that plant community composition is important both for food web structure and biological carbon sequestration. This seems likely to also be true for phytoplankton, but their small size makes the routine identification (i.e., based on light microscopy) of different plankton communities difficult. Using changes in size structure (established through size fractionated chlorophyll analysis) of phytoplankton communities as a proxy for changes in community diversity, it has been shown that differences in photosynthetic parameters²⁵, responses to nutrient availability²⁶, temperature²⁷ and ocean-atmosphere carbon flux²⁸ can all be related to community diversity. F_v/F_m^* is to some degree dependent on species composition²⁹ and does not, therefore, provide a quantitative indicator of community size structure. Nevertheless, if the general relationship noted here is found to be ubiquitous, then F_v/F_m^* could potentially become a valuable tool for exploring differences in phytoplankton community distributions in nature.

Both the vertical chlorophyll distributions (Fig. 2) and the F_v/F_m^* distributions (Fig. 3) found were consistent with the conclusion^{12,13} of vertical mixing occurring at the shelf edge. It seemed that the water column stability characteristics allowing the development of distinct DCMs north and south of the shelf edge were not present at the shelf edge. Elevated F_v/F_m^* values suggest a relaxation of nutrient depletion in the ambient phytoplankton community, so the surface phytoplankton communities appeared to be more nutrient replete over the shelf edge than their counterparts to the north and south (although at the extremes of some of the transects other than shelf edge mixing processes appear also to influence surface F_v/F_m^* and phytoplankton size structure, see Fig. 3).

Elevated F_v/F_m^* was shown here to be associated with increasing dominance of large cells in the phytoplankton community (Fig. 4). Using F_v/F_m^* as an indicator for community size structure, we conclude that communities dominated by larger photosynthetic organisms were found at the DCM and throughout the water column where vertical mixing is suggested to occur. Thus, we can predict greater retention (i.e., capture, ingestion) efficiency of the phytoplankton by the larger zooplankton grazers in these areas.

Copepod egg production depends on numerous factors, where food availability, type and quality are of importance³⁰. It is believed that copepod egg production relates directly to food intake and that copepod retention of food particles greatly increases when particle size is $> 10 \mu\text{m}$ ³¹. We therefore suggest that enhanced EPR (Fig. 5) and predominance of large copepods (Fig. 6) at the shelf edge were related to a higher proportion of large phytoplankton. However, a time lag, and thus a spatial mismatch due to current activity³², between greater food retention and EPR may be expected. This may be reflected in the lack of linear relationship between EPR and percentage of large cells in the phytoplankton community (see Supplementary Fig. S3 online).

The overall findings of a response signal in planktonic communities to vertical mixing provide empirical evidence that physical characteristics of shelf fronts have the potential to provide food requirements necessary for fish larvae survival¹⁴ and thus fuel the production of higher trophic levels. Interestingly, pelagic fishing intensity in the Celtic Sea is concentrated at the edge of the continental shelf, which was suggested to be caused by internal tides¹⁹ that could in turn lead to NP. We therefore speculate that our results can explain the accumulation of organisms representing higher trophic levels in our study area¹⁵.

Conclusion

This study demonstrates sub-mesoscale differences in phytoplankton community size structure that appear to influence both zooplankton distributions and egg production. Geographically, these differences in phytoplankton community structure were associated with a region where episodic upwelling of nutrient-rich deep water to the euphotic zone is known to exist. A causal link between this upwelling and the differences noted in community size structure was suggested by the significant positive relationship between F_v/F_m^* and dominance of larger phytoplankton in the community, as higher values indicate a relaxation of nutrient depletion. The increased copepod egg production and dominance of larger cells in the phytoplankton community at the shelf edge further suggested a signal propagating from the localised upwelling to higher trophic levels. We suggest that such upwelling-induced sub-mesoscale differences in the structure of plankton ecosystems may be an underlying driver of “patchiness” in the distribution of marine organisms at even higher trophic levels^{15,19,33}.

Methods

Study area

The VERMIX cruise (12–31 July 2016) in the northeastern North Sea sampled along five transects (Tr.1–5) and F_v/F_m measurements were taken on Tr. 2–5 and were used for the phytoplankton analyses. Measurements of turbulence, hydrography, nutrients and chlorophyll *a* distributions and sampling conditions were described in a previous study¹². Measurements of nitrate and phosphate¹² suggest that denitrification might be occurring in the shallow area ($< \sim 60 \text{ m}$) south of the shelf edge towards the central North Sea. More recently, the shallow and the shelf edge area were shown to be weakly connected whereas a larger connectivity was found between the shelf edge and water above the Norwegian trench²⁸. Therefore, we refer to visited stations in three groups: *shallow* ($< 60 \text{ m}$), *shelf edge* (60–120 m), and *deep* ($> 120 \text{ m}$), as defined in a previous study¹³.

F_v/F_m corrected for photoinhibition (F_v/F_m^*)

At each station, water was collected from 4 selected depths for determination of chlorophyll *a* fluorescence kinetics, transferred directly to a 300 ml dark glass flask and stored for $\sim 30 \text{ min}$ until measurement of F_v/F_m . Subsequently, 100 ml of sample were transferred to a 200 ml transparent glass flask and incubated for $\sim 4 \text{ h}$ at

50 $\mu\text{mol photons m}^{-2} \text{ s}^{-1}$ in a temperature-controlled room, with a temperature adjusted to match the average temperature of the collected water samples. This light treatment has been shown to remove any signal in the F_v/F_m caused by photoinhibition¹⁸. After the incubation, F_v/F_m was again determined. Differences in post-incubation F_v/F_m were assumed to reflect differences in nutrient status in the phytoplankton communities with low F_v/F_m^* values indicating nutrient stress.

F_v/F_m was measured using a FastOcean FRRf 3 sensor (Chelsea Technologies Group, UK) with a dark chamber installed, and data was acquired in the FASTpro 8 software (Chelsea Technologies Group, UK). A single turnover protocol was used with a saturation phase consisting of 100 flashlets with a 2 μs pitch and 16 sequence repetitions. For each measurement, the sensitivity (PMT eht) was automatically optimised by the software and the LED light intensity (E_{LED}) was manually optimised. The saturating light was composed of 450, 530, and 624 nm wavelengths in a constant ratio of 1:0.5:0.8. The detection limit of the system was $F_v/F_m = 0.15$. All values below the detection limit were presented as 0.15 here. For depths < 30 m, the highest F_v/F_m value (dark/light incubated) was presented to reflect the maximum PSII electron transport potential. For depths > 30 m, the F_v/F_m as a result of dark incubation only was presented as no photoinhibition was expected at these depths.

Chlorophyll

Total chlorophyll *a* and size fractions of chlorophyll *a* were determined at selected stations at 5 m, the depth of the deep chlorophyll *a* maximum (DCM) and at 30 m. Seawater samples tapped from Niskin bottles and filtered through Whatman GFF (0.7), 3, and 10 μm pore size Millipore filters. For each sampling depth and filter size, triplicate filtrations of 200–500 ml seawater for the GFF filters and 400–1000 ml seawater for the 3 and 10 μm filters were performed. The samples were immediately frozen and later extracted for a minimum of 6 h in 5 ml ethanol (96%) in the dark at 6 °C. Chlorophyll *a* concentrations were measured using a Trilogy Laboratory Fluorometer (Turner Designs, CA, USA), which had been calibrated using a chlorophyll *a* standard from the DHI Group (Hørsholm, Denmark).

Copepod egg production rate (EPR)

Centropages typicus and *Temora longicornis* females were collected at 23 stations with a 180 μm mesh plankton net, (1 m, ring diameter) fitted with a 5 L non-filtering cod-end. The sampling depth was about 2 m under the DCM and the net was towed vertically with a towing speed of approximately 15 m per minute.

The contents of the cod-end were gently transferred into a bucket with surface (5 m) water from the respective stations. Immediately after sampling, 20 active undamaged females were selected under a stereomicroscope and introduced into 250 ml bottles (1–3 females per bottle) filled with 64 μm screened ambient water. Four to 11 replicates were incubated per station. Screening was done in order to remove all eggs and nauplii from the initial incubation water. Females were incubated in darkness for 24 h at temperatures appropriate for the ambient temperature at the station where they were collected. The incubation was terminated by filtering the content of the bottles onto a 20 μm sieve and then washing the sieve contents into a small Petri-dish. Females were then removed and measured for length and the eggs counted.

Zooplankton sampling and processing

Zooplankton samples were collected at 14 stations (latitudes ranging between 56.65–57.83°N and longitudes between 6.28–8.25°E) (See Supplementary Table S1 online) using a Multinet (Hydro-Bios, Kiel; mesh size 200 μm). Zooplankton were stored in 4% formalin in the freezer. Samples were size fractionated using a sieve and zooplankton split into two size groups, > 640 μm and < 640 μm . Samples were then digitally scanned on an Epson Perfection V800 photo (2400 dpi, 16 bit gray), using the software Vuescan (version 9.5, <https://www.hamrick.com/>). In total, 1340 images were produced, representing 134 samples (5 images for each sub-sample). Images were processed and statistics with the zooimage package³⁴ and after the creation of a classifier, individuals were automatically identified, counted.

Raw scanned images were processed using ImageJ software (version 1.52, <https://imagej.net/ij/>) through the zooimage plugin “Scanner_Gray16”. Sub-images called vignettes were produced, representing every organism or particle detected by the plugin. Given the large diversity of zooplankton, a reasonable trade-off between taxonomy identification and resolution was needed to reduce errors³⁵. The training set was composed of ten representative samples randomly chosen (different depths and transects) to be classified manually. Vignettes were grouped per class through the Xnview software (version 2.30). The classifier was assessed by the calculation of a tenfold cross-validation between the manual and automated classifications (Fig. S1). Additional tests were completed through an analysis of the precision and recall F-score ratios, and a manual validation of the classifier. The final classifier had a global error of 7.2% ($F = 0.91$).

Abundance per size (Equivalent Circular Diameter (ECD)) spectra (< 0.5, 0.5–1, 1–1.5, 1.5–2 and 2–2.5 mm) was obtained on copepods taxa. The size spectra 0.5–1 mm and 1.5–2 mm were consistently the most abundant groups in the samples. Therefore, subsequent analyses were conducted on these two size spectra which were assumed to be representative of the copepod communities in the area.

Data availability

The datasets generated during the study are available in the supplementary information files.

Received: 10 February 2024; Accepted: 17 December 2024

Published online: 07 January 2025

References

- Bainbridge, R. The size, shape and density of marine phytoplankton. *Biol. Rev.* **32**, 91–115. <https://doi.org/10.1111/j.1469-185X.1957.tb01577.x> (1957).
- Hauray, L. R., McGowan, J. A. & Wiebe, P. H. Patterns and processes in the time-space scales of plankton distributions. In *Spatial Pattern in Plankton Communities* (ed. Steele, J. H.) (Springer, 1978).
- Folt, C. L. & Burns, C. W. Biological drivers of zooplankton patchiness. *Trends Ecol. Evol.* **14**, 300–305. [https://doi.org/10.1016/S0169-5347\(99\)01616-X](https://doi.org/10.1016/S0169-5347(99)01616-X) (1999).
- Cushing, D. H. A difference in structure between ecosystems in strongly stratified waters and in those that are only weakly stratified. *J. Plankton Res.* **11**, 1–13. <https://doi.org/10.1093/plankt/11.1.1> (1989).
- Kiorboe, T. Turbulence, phytoplankton cell size, and the structure of pelagic food webs. *Adv. Mar. Biol.* **29**, 1–72. [https://doi.org/10.1016/S0065-2881\(08\)60129-7](https://doi.org/10.1016/S0065-2881(08)60129-7) (1993).
- Flint, M. V., Sukhanova, I. N., Kopylov, A. I., Poyarkov, S. G. & Whitedge, T. E. Plankton distribution associated with frontal zones in the vicinity of the Pribilof Islands. *Deep Sea Res. Part II Top. Stud. Oceanogr.* **49**, 6069–6093. [https://doi.org/10.1016/S0967-0645\(02\)00334-X](https://doi.org/10.1016/S0967-0645(02)00334-X) (2002).
- Munk, P., Larsson, P., Danielsen, D. & Moksness, E. Variability in frontal zone formation and distribution of gadoid fish larvae at the shelf break in the northeastern North Sea. *Mar. Ecol. Prog. Ser.* **177**, 221–233. <https://doi.org/10.3354/meps177221> (1999).
- Godø, O. R. et al. Mesoscale eddies are oases for higher trophic marine life. *PLoS One* **7**, e30161. <https://doi.org/10.1371/journal.pone.0030161> (2012).
- Dugdale, R. C. & Goering, J. J. Uptake of new and regenerated forms of nitrogen in primary productivity. *Limnol. Oceanogr.* **12**, 196–206. <https://doi.org/10.4319/lo.1967.12.2.0196> (1967).
- Eppey, R. W. & Peterson, B. J. Particulate organic matter flux and planktonic new production in the deep ocean. *Nature* **282**, 677–680. <https://doi.org/10.1038/282677a0> (1979).
- Richardson, K. et al. Localised mixing and heterogeneity in the plankton food web in a frontal region of the Sargasso Sea: implications for eel early life history?. *Mar. Ecol. Prog. Ser.* **504**, 91–107. <https://doi.org/10.3354/meps10766> (2014).
- Bendtsen, J. & Richardson, K. Turbulence measurements suggest high rates of new production over the shelf edge in the northeastern North Sea during summer. *Biogeosciences* **15**, 7315–7332. <https://doi.org/10.5194/bg-2018-385> (2018).
- Bendtsen, J. & Richardson, K. New production across the shelf-edge in the northeastern North Sea during the stratified summer period. *J. Mar. Syst.* **211**, 103414. <https://doi.org/10.1016/j.jmarsys.2020.103414> (2020).
- Munk, P. Fish larvae at fronts: Horizontal and vertical distributions of gadoid fish larvae across a frontal zone at the Norwegian Trench. *Deep Sea Res. Part II Top. Stud. Oceanogr.* **107**, 3–14. <https://doi.org/10.1016/j.dsr2.2014.01.016> (2014).
- Sveegaard, S. et al. High-density areas for harbor porpoises (*Phocoena phocoena*) identified by satellite tracking. *Mar. Mammal Sci.* **27**, 230–246. <https://doi.org/10.1111/j.1748-7692.2010.00379.x> (2011).
- García-Comas, C. et al. Prey size diversity hinders biomass trophic transfer and predator size diversity promotes it in planktonic communities. *Proc. R. Soc. B* **283**, 20152129 (2016).
- Reid, D. G. SEFOS—Shelf edge fisheries and oceanography studies: an overview. *Fisheries Res.* **50**, 1–15. [https://doi.org/10.1016/S0165-7836\(00\)00238-1](https://doi.org/10.1016/S0165-7836(00)00238-1) (2001).
- ICES. Working group on widely distributed stocks (WGWIDE). *ICES Sci. Rep.* **5**, 82. <https://doi.org/10.17895/ices.pub.24025482.v1> (2023).
- Sharples, J., Ellis, J. R., Nolan, G. & Scott, B. E. Fishing and the oceanography of a stratified shelf sea. *Prog. Oceanogr.* **117**, 130–139. <https://doi.org/10.1016/j.pocean.2013.06.014> (2013).
- Legendre, L. The significance of microalgal blooms for fisheries and for the export of particulate organic carbon in oceans. *J. Plankton Res.* **12**, 681–699. <https://doi.org/10.1093/plankt/12.4.681> (1990).
- Ryther, J. H. Photosynthesis and fish production in the Sea. *Science* **166**, 72–76. <https://doi.org/10.1126/science.166.3901.72> (1969).
- From, N., Richardson, K., Mousing, E. A. & Jensen, P. E. Removing the light history signal from normalized variable fluorescence (F_v/F_m) measurements on marine phytoplankton. *Limnol. Oceanogr. Methods* **12**, 776–783. <https://doi.org/10.4319/lom.2014.12.776> (2014).
- Vihtakari, M. ggOceanMaps: Plot Data on Oceanographic Maps using ggplot2. R package version 2.2.1. <https://mikkovihtakari.github.io/ggOceanMaps/> (2023).
- R Core Team. R: A Language and Environment for Statistical Computing. <https://www.r-project.org/> (R Foundation for Statistical Computing, 2023).
- Richardson, K., Bendtsen, J., Kragh, T. & Mousing, E. A. Constraining the distribution of photosynthetic parameters in the global ocean. *Front. Mar. Sci.* **3**, 269. <https://doi.org/10.3389/fmars.2016.00269> (2016).
- Mousing, E. A., Richardson, K. & Ellegaard, M. Global patterns in phytoplankton biomass and community size structure in relation to macronutrients in the open ocean. *Limnol. Oceanogr.* **63**, 1298–1312. <https://doi.org/10.1002/lno.10772> (2018).
- Mousing, E. A., Ellegaard, M. & Richardson, K. Global patterns in phytoplankton community size structure—Evidence for a direct temperature effect. *Mar. Ecol. Prog. Ser.* **497**, 25–38. <https://doi.org/10.3354/meps10583> (2014).
- Hilligsøe, K. M. et al. Linking phytoplankton community size composition with temperature, plankton food web structure and sea-air CO₂ flux. *Deep Sea Res. Part Oceanogr. Res. Pap.* **58**, 826–838. <https://doi.org/10.1016/j.dsr.2011.06.004> (2011).
- Suggett, D., Moore, M., Hickman, A. & Geider, R. Interpretation of fast repetition rate (FRR) fluorescence: Signatures of phytoplankton community structure versus physiological state. *Mar. Ecol. Prog. Ser.* **376**, 1–19. <https://doi.org/10.3354/meps07830> (2009).
- Jonasdottir, S., Visser, A. & Jespersen, C. Assessing the role of food quality in the production and hatching of *Temora longicornis* eggs. *Mar. Ecol. Prog. Ser.* **382**, 139–150. <https://doi.org/10.3354/meps07985> (2009).
- Traboni, C., Calbet, A. & Saiz, E. Effects of prey trophic mode on the gross-growth efficiency of marine copepods: the case of mixoplankton. *Sci. Rep.* **10**, 12259. <https://doi.org/10.1038/s41598-020-69174-w> (2020).
- Bendtsen, J., Sørensen, L. L., Daugbjerg, N., Lundholm, N. & Richardson, K. Phytoplankton diversity explained by connectivity across a mesoscale frontal system in the open ocean. *Sci. Rep.* **13**, 12117. <https://doi.org/10.1038/s41598-023-38831-1> (2023).
- Runge, J. A. Should we expect a relationship between primary production and fisheries? The role of copepod dynamics as a filter of trophic variability. *Hydrobiologia* **167**(168), 61–71. https://doi.org/10.1007/978-94-009-3103-9_6 (1988).
- Phillippe, G. & Kevin, D. Supervised classification of images, applied to plankton samples using R and Zooimage. *Data Min. Appl. R* <https://doi.org/10.1016/B978-0-12-411511-8.00013-X> (2014).
- Gislason, A. & Silva, T. Comparison between automated analysis of zooplankton using ZooImage and traditional methodology. *J. Plankton Res.* **31**, 1505–1516. <https://doi.org/10.1093/plankt/fbp094> (2009).

Acknowledgements

We thank the captain and crew of the R/V Dana for helpful assistance during the cruise and Eik Ehlert Britch for technical support. The VERMIX cruise was supported by funding for ship-time by the Danish Centre for Marine Research. The Velux Foundations (Grant No. 00013281) provided support for the analysis of the measurements. The Carlsberg foundation provided support for the turbulence instrument (CF15-0301). This study was also

supported by the Danish National Science Foundation via its support of the Centre for Macroecology, Evolution, and Climate (Grant No. DNRF96).

Author contributions

AC did the zooplankton analyses and the analyses demonstrating links between different ecosystem components. She also drafted the manuscript. JB was responsible for the turbulence and hydrographic data collection and analyses. SHJ was responsible for the copepod egg production experiments and supervised the zooplankton identification. EAM was responsible for carrying out the size fractionation of chlorophyll and ND for chlorophyll analyses. NF carried out the Fv/Fm measurements. JTC collected the zooplankton samples. TS supervised the use of zooimage to determine zooplankton composition. KR planned the study and was cruise leader. She also supervised the analysis and drafting of the manuscript. All authors have read and commented on the manuscript.

Declarations

Competing interests

The authors declare no competing interests.

Additional information

Supplementary Information The online version contains supplementary material available at <https://doi.org/10.1038/s41598-024-83811-8>.

Correspondence and requests for materials should be addressed to A.C.

Reprints and permissions information is available at www.nature.com/reprints.

Publisher's note Springer Nature remains neutral with regard to jurisdictional claims in published maps and institutional affiliations.

Open Access This article is licensed under a Creative Commons Attribution 4.0 International License, which permits use, sharing, adaptation, distribution and reproduction in any medium or format, as long as you give appropriate credit to the original author(s) and the source, provide a link to the Creative Commons licence, and indicate if changes were made. The images or other third party material in this article are included in the article's Creative Commons licence, unless indicated otherwise in a credit line to the material. If material is not included in the article's Creative Commons licence and your intended use is not permitted by statutory regulation or exceeds the permitted use, you will need to obtain permission directly from the copyright holder. To view a copy of this licence, visit <http://creativecommons.org/licenses/by/4.0/>.

© The Author(s) 2025